Investigations of radiation pressure : optical side-band cooling of a trampoline resonator and the effect of superconductivity on the Casimir force

Eerkens, H.J.

3

Parametric Amplification of the Motion of an Optomechanical Resonator

The interaction between light and a mechanical oscillator influences the phase of the light and the motion of the oscillator. Whether the oscillator is damped or driven depends on the phase of the force introduced by the light relative to the phase of the mechanical motion. The oscillator can be damped by differentiating the motion read-out signal and then feeding back this signal by modulating the light, comparable to pushing a child on a swing. This interaction not only damps the motion, but due to the low noise of the light source also effectively cools the oscillator. This method is therefore known as active feedback cooling. Active feedback cooling was already demonstrated by using electronic read-out [66, 67] or by optical read-out [7, 68, 69].

When the light used to read out the motion of the oscillator is contained in an optomechanical cavity, the interaction between the light and mechanical oscillator enters a vicious circle where the light influences the mechanical motion, which influence the phase of the light, which influences the mechanical motion again, etcetera. The system is now described as a parametric oscillator, where the mechanical resonator is driven or damped by varying one of the parameters of the system. This can be compared to a child that pushes itself on a swing by varying the swing's moment of inertia [70]. This passive cavity cooling of a mechanical oscillator has also been demonstrated multiple times [25, 71, 72]. Instead of monitoring and altering the phase of the light, cooling is now possible by changing the frequency of the laser light with respect to the cavity resonance. Optical cooling occurs when the laser is detuned to the red side of the resonance, below the cavity frequency.

At the blue side-band, the oscillator is driven which can lead to parametric instabilities [73], self-induced oscillations [74] and even chaos [75, 76]. The theoretical framework for this behaviour has also been developed [77, 78] and introduces an attractor diagram [79] that gives an overview of the optomechanical gain of the system

This chapter is based on: F. M. Buters, H. J. Eerkens, K. Heeck, M. J. Weaver, B. Pepper, P. Sonin, S. de Man and D. Bouwmeester, "Large parametric amplification in an optomechanical system," *Phys. Scr.*, **T165**, 014003, (2015).

as a function of the mirror amplitude and the laser detuning. This attractor diagram can be explored experimentally [80] and shows that at higher oscillator amplitude driving (cooling) is not restricted to the blue (red) side of the cavity resonance. In this chapter we will show large parametric amplification of our mirror motion, leading to self-induced oscillations without the appearance of chaotic motion even at large amplitudes [81].

3.1 Parametric oscillations

When the frequency of a laser is scanned across the resonance of an optomechanical cavity, the resonance peak shows up in the transmission signal read out by a photodetector. However, when the laser power is large enough and the frequency scan rate slow enough, not only the main resonance is visible, but also several side-bands appear at multiples of the mechanical resonance frequency Ω_m. An example of this transmission signal is shown in Figure 3.1, which shows the transmitted intensity as a function of the laser detuning $\Delta = \omega_{\text{laser}} - \omega_{\text{cav}}$, normalized to the mechanical frequency. Here we introduce the angular frequencies ω_{laser} and ω_{cav} for the laser and cavity respectively.

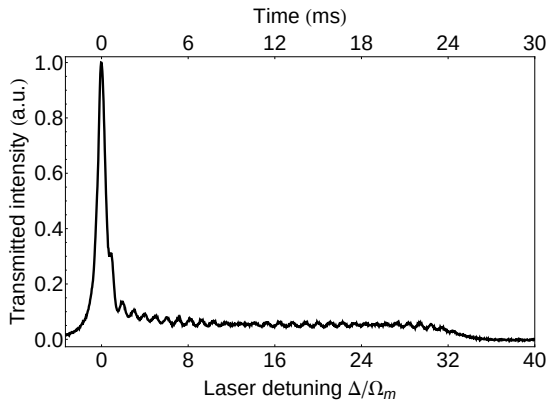

Figure 3.1: Transmission signal of a linear frequency sweep across an optomechanical cavity, the main cavity resonance is visible as well as side-bands spaced at the mechanical frequency. These side-bands are a result of parametric driving of the mechanical oscillator, while its increased amplitude creates stronger modulation of the amplitude field, which in turn allows even more driving of the oscillator.

We can understand the appearance of the side-bands with the following explanation. As the laser is scanned across the cavity resonance at ω_{cav}, the resonance peak is visible in transmission. The interaction with the mirror results in Stokes and anti-Stokes side-bands located at $\omega_{\text{cav}} \pm \Omega_m$. Here we assume that the amplitude of the mirror oscillation is small, such that no higher order side-bands are formed. The cavity light interferes with the incoming laser light, which creates a force at Ω_m acting on the mirror. However, since the side-bands appear at both sides of the cavity,

this force both damps and drives the mirror, such that in effect the mirror motion remains unaltered. The laser is then scanned slowly towards the blue side-band, at which point the interaction with the mirror results in side-bands at ω_{cav} and at $\omega_{\text{cav}} + 2\Omega_m$. The first side-bands is resonant with the cavity field and is enhanced, while the second is suppressed. Since the interference of the laser light with the cavity field now only results in a driving force, the mirror amplitude is increased. This leads to a stronger optical field modulation, which in turn increases the amplitude even further, leading to an even stronger modulation, until a balance is reached. This is known as limit cycle behaviour. The laser is then detuned even further, while the larger mechanical amplitude allows the creation of increasingly more side-bands. During the sweep, the Stokes side-bands are enhanced, while the anti-Stokes side-bands remain suppressed, driving the mirror when the detuning is at multiples of the mechanical frequency.

This whole process is known as parametric amplification of the resonator, since it is induced by a change in the parameters of the system. It continues until the power loss due to friction in the system is no longer balanced by the power put into the system via the laser light. The mirror amplitude is then no longer increased and reduces to its original value given by the thermal motion of the mirror. When the laser is set back to a frequency below the cavity resonance frequency, the sweep can be repeated, leading to the same output field. Note that this parametric amplification, despite similar appearances, should not be confused with optical ringing in a high-finesse Fabry-Perot cavity [82].

3.2 Description of the set-up

Our optomechanical system is an $L = 5\,\text{cm}$ long confocal optical cavity where a trampoline resonator forms one of the end mirrors. The trampoline resonator consists of a Bragg mirror with diameter $60\,\mu\text{m}$ attached via four Si_3N_4 wires to a silicon substrate [63]. The motion of interest is the fundamental mechanical mode with a resonance frequency of $\Omega_m/2\pi = 300\,\text{kHz}$. A schematic of the set-up is given in Figure 3.2.

The light from a CW Nd:YAG laser (Coherent Mephisto) with a wavelength $\lambda = 1064\,\text{nm}$ passes through an optical isolator to avoid back reflections and an electro-optic phase modulator (EOM) tuned at $9.5\,\text{MHz}$ that is used for calibration of the detuning. The light is coupled into an optical fiber that transports it into a vacuum chamber which contains the optomechanical cavity. Most of the experiments were done at a background pressure of 10^{-6} mbar. To avoid mechanical noise, a vibration isolation system containing several Eddy-current dampers decouples the optomechanical cavity from the outside world.

The laser frequency can be tuned via a piezo on the laser crystal, with a typical scan speed of $100 - 400\,\text{MHz/s}$, which is slow compared to the cavity life time. The light from the cavity, imprinted with the motion of the trampoline resonator, is detected by two photodetectors placed in transmission and, via an optical circulator, in reflection. The data is acquired by a digital oscilloscope (Agilent DSO-X 2004A).

The experimental parameters of our optomechanical cavity were determined sep-

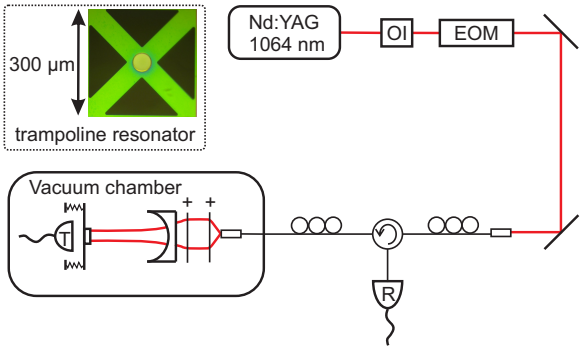

Figure 3.2: Schematic of the experimental set-up; the light of a Nd:YAG laser operating around $1064\,\text{nm}$ is coupled into a single mode optical fiber and propagates via an optical circulator to our optomechanical cavity, which is placed inside a vacuum chamber. The transmitted light falls onto a photodetector and the reflected light is detected after passing the circulator again. The electro-optic modulator (EOM) tuned at $9.5\,\text{MHz}$ is used to calibrate the detuning of the laser frequency with respect to the cavity. The inset shows an optical image of the trampoline resonator.

arately. The cavity linewidth $\kappa/2\pi = 300\,\text{kHz}$ was obtained from an optical ring-down measurement and from the thermal mechanical noise spectrum we could determine a mechanical linewidth of $\Gamma_m/2\pi = 8.8\,\text{Hz}$ at the background pressure of $10^{-6}\,\text{mbar}$. This corresponds to a mechanical quality factor of $Q_m = 34000$. The intrinsic linewidth can be altered by changing the background pressure in the vacuum chamber.

3.3 Comparison to simulations

To better understand our experimental results, we compare it with simulations based on the equations of the system. There are two coupled equations of motion for our optomechanical cavity, the first describes the optical field in the cavity α and the second the displacement x of the oscillator. We have neglected thermal and mechanical noise sources.

$$\dot{\alpha}(t) = -\frac{\kappa}{2}\alpha(t) + \mathrm{i}(\Delta + Gx(t))\alpha(t) + \sqrt{\kappa_{\text{ex}}}\alpha_{\text{in}}, \tag{3.1}$$

$$\ddot{x}(t) = -\Omega_m^2 x(t) - \Gamma_m \dot{x}(t) + \frac{\hbar G}{m_{\text{eff}}}|\alpha(t)^2|, \tag{3.2}$$

here the dot indicates the time-derivative. The other parameters are as follows: $G = \omega_{\text{cav}}/L$ the optical frequency shift per displacement, the cavity coupling loss rate $\kappa_{\text{ex}}/2\pi = 50\,\text{kHz}$, α_{in} the laser field, $\hbar$ the reduced Planck constant and $m_{\text{eff}} = 110 \times 10^{-12}\,\text{kg}$ the effective mass of the mechanical mode. By solving these equations of motion, we can give a more quantitative understanding of our parametric oscillator.

The motion of the mechanical oscillator is partly determined by its effective damping rate which is a sum of the intrinsic linewidth and the optomechanical damping rate $\Gamma_{\text{eff}} = \Gamma_m + \Gamma_{\text{opt}}$. An expression for Γ_{opt} in terms of the optical field and the amplitude A of the oscillator is deduced from the equation above [83]:

$$\Gamma_{\text{opt}}(A) = \frac{2\hbar G \kappa_{\text{ex}} \alpha_{\text{in}}^2}{m_{\text{eff}} \Omega_m A} \text{Im}\left(\sum_n \alpha_{n+1}^* \alpha_n\right), \tag{3.3}$$

$$\alpha_n = \frac{J_n(-GA/\Omega_m)}{\kappa/2 - \text{i}\tilde{\Delta} + \text{i}n\Omega_m}, \tag{3.4}$$

where $J_n(x)$ is the Bessel function of the first kind and $\tilde{\Delta} = \omega_{\text{laser}} - \omega_{\text{cav}} + G\bar{x}$ is the effective laser detuning which also accounts for the static displacement $\bar{x}$ of the mirror due to radiation pressure. This static displacement is small enough that we can neglect it, such that $\tilde{\Delta} \approx \Delta$.

The harmonics in the optical field are indicated by α_n for the nth harmonic. They are created by the mirror motion, which phase modulates the incoming laser light via the term $Gx(t)\alpha(t)$ in Eq. 3.1. The modulation depth is given by the argument of the Bessel function, $\phi_0 = -GA/\Omega_m$, and determines the number of side-bands that appear at frequencies $\omega = \omega_{\text{laser}} \pm n\Omega_m$. Note that the thermally excited mirror amplitude at 300 K is already sufficient to create a side-band, but more side-bands are created as the amplitude increases and more harmonics of the mechanical frequency Ω_m are imprinted on the cavity field. These side-bands are scaled by the cavity line shape as the denominator in Eq. 3.4 indicates. The modulated cavity field interacts again with the mirror, via the radiation pressure proportional to the cavity intensity $|\alpha^2|$, see Eq. 3.2. But the mirror only reacts to components of the force at the mechanical frequency, which are formed by the mixing at the moving mirror of two consecutive side-bands, $\sum_n \alpha_{n+1}^* \alpha_n$. The real part of this sum is responsible for the optical spring effect. But we are interested in optical damping or driving, which is described by the imaginary part of the sum, as is shown in Eq. 3.3.

When the optomechanical damping rate Γ_{opt} is larger than zero, the mechanical oscillator is damped and effectively cooled. But the optomechanical damping rate can also be negative. When the optomechanical damping rate overcomes the intrinsic mechanical linewidth, such that the effective linewidth is negative, self-induced oscillations occur. This is better expressed in terms of the optomechanical gain [83]:

$$\zeta_{\text{opt}} = -\frac{\Gamma_{\text{opt}}}{\Gamma_m} = \frac{P_{\text{rad}}}{P_{\text{fric}}} \tag{3.5}$$

with P_{rad} the power in the radiation pressure acting on the mirror motion, that can either be extracted from the oscillator or delivered to it. P_{fric} is the power lost from the oscillator via friction. From the ratio in Γ_{opt} and Γ_m we see that damping and cooling occurs when the optomechanical gain is smaller than zero, in this case the radiation pressure extracts power from the oscillator. Parametric oscillations occur when more power is added to the resonator than can be drained via friction, so when $\zeta_{\text{opt}} > 1$. In this situation Γ_{opt} is negative and has a larger magnitude than Γ_m, in accordance with what was mentioned before. In the intermediate regime

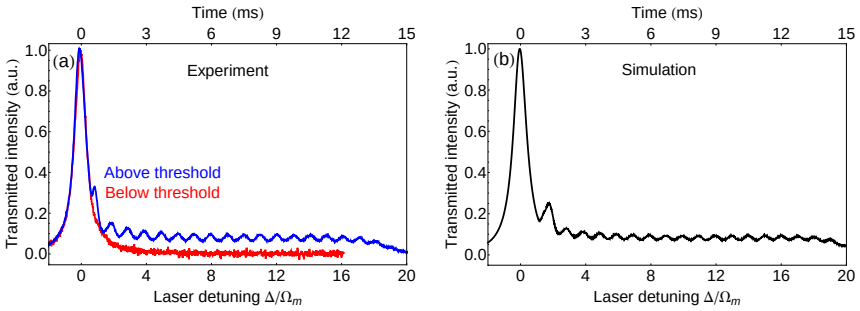

Figure 3.3: Linear frequency sweep across an optomechanical cavity resonance: (a) Experimental results below (red line) and above (blue line) the power threshold, with a mechanical quality factor $Q_m = 7300$ and scan speed $400\,\text{MHz/s}$; (b) Simulation based on the equations of motion of the system, with input the thermal amplitude of the mirror motion at $300\,\text{K}$.

$0 \leq \zeta_{\text{opt}} < 1$ the linewidth of the oscillator is reduced, but not enough for parametric oscillations to occur.

Parametric oscillations occur only above a certain power threshold, when $P_{\text{rad}} > P_{\text{fric}}$. Self-induced oscillations are therefore also known as mechanical or phonon lasing [25]. The effect of the power threshold is visible in Figure 3.3(a), which shows the experimental results of two linear frequency sweeps with a scan speed of $400\,\text{MHz/s}$. The two sweeps were obtained at different laser powers. No parametric oscillations occur below the power threshold, while above the power threshold oscillations continue to a detuning of $\Delta = 19\Omega_m$. The numerical simulations in Figure 3.3(b) are obtained by solving the two equations of motion, Eqs. 3.1 and 3.2. As input parameters we used $\alpha(0) = 0$, $\dot{\alpha}(0) = 0$, $x(0) = x_0$ and $\dot{x}(0) = 0$, with x_0 the thermally excited mirror amplitude at $300\,\text{K}$. In the simulations, the laser detuning is varied linearly across the cavity resonance while the laser power was kept constant. The simulations show excellent agreement with our experimental results above the power threshold.

When we zoom in at the optical side-bands, we should see the harmonics of the mechanical frequency imprinted on the cavity field [79]. Since our photodetector in transmission is not fast enough to see these fast modulations, we use the reflection detector. The numerical simulations are also computed in reflection. Both the numerical and experimental results are shown in Figure 3.4, for different values of the detuning. As we can see, the number of harmonics increases with larger detuning and therefore with larger amplitude of the mirror. The striking resemblance between simulations and experiment is another indication of the quality of the experimental set-up.

The self-induced oscillations occur as long as the optomechanical gain defined in Eq. 3.5 is larger than one. An indicator of the duration of the parametric oscillations is the amount of side-bands that are created. According to the definition of the optomechanical gain, this plateau length should be linear in the laser power, above a certain threshold, and inversely proportional to the mechanical linewidth. The effect of laser power is shown in Figure 3.5(a), where we have plotted the plateau length

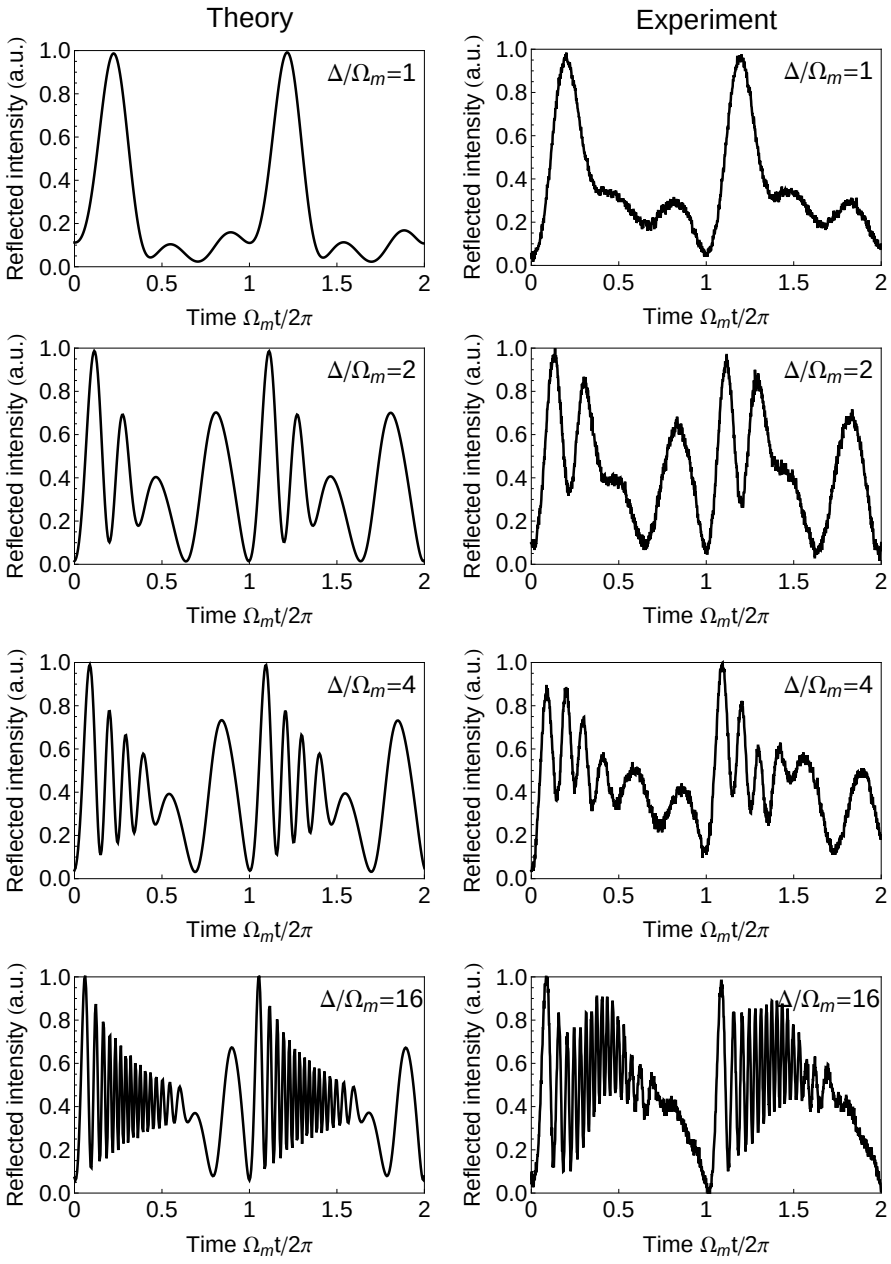

Figure 3.4: Imprint of the mechanical motion as harmonics of the mechanical frequency Ω_m on the reflected cavity field. Simulations based on solving Eqs. 3.1 and 3.2 are shown in the left column at different detunings, the experimental results at the same detuning are shown in the right column.

for different laser input powers (blue dots). There are no parametric oscillations until the power is increased enough, after which the plateau length increases linear with power. The red line is a fit to the expression in Eq. 3.5.

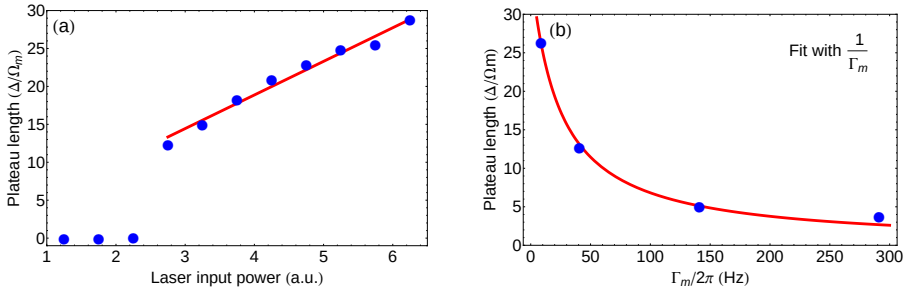

Figure 3.5: Plateau length as an indication of the optomechanical gain, the blue dots mark the amount of side-bands under different experimental conditions, the red line is a fit of the optomechanical gain: (a) Above a certain power threshold, the optomechanical gain is linear in the laser power; (b) The optomechanical gain is inversely proportional to the intrinsic mechanical linewidth.

To measure the influence of the mechanical linewidth, we have increased the background pressure in the vacuum chamber. For four different pressures, resulting in four different values of Γ_m, but at constant laser power, we have determined the plateau length, see Figure 3.5(b). The fit to ζ_{opt} shows that it is indeed inversely proportional to the mechanical linewidth. We can therefore conclude that the optomechanical gain shows the expected behaviour.

3.4 No transition to chaotic motion

We have shown that the two equation of motions introduced in Eqs. 3.1 and 3.2 are sufficient to describe the observed self-induced oscillations. When we take another look at Figure 3.1, we see parametric oscillations up to a detuning of $\Delta = 32\Omega_m$. The amplitude of the mirror at this point is found, by solving $\zeta_{\text{opt}}(\Delta = 32\Omega_m, A) < 1$, to be 450 times larger than the thermally excited mirror amplitude at 300 K.

In other systems, such high increase in amplitude is often not reached due to the transition to chaotic motion [75, 76], induced either by an extra photothermal force due to heating induced expansion of the mirror, or by the influence of outside vibrations. The absence of chaos in our system is a result of our high-quality mirror coatings with low absorption and of our good mechanical isolation from the environment. This opens the possibility of optical stabilization of the mirror at large amplitudes to greatly enhance the sensitivity when the optomechanical set-up is used for force detection [84].